NIH Public Access
Author Manuscript
Biochemistry. Author manuscript; available in PMC 2013 January 23.

Published in final edited form as:
Biochemistry. 2011 December 13; 50(49): 10598–10606. doi:10.1021/bi201351d.

Reconstitution of Platelet Glycoprotein Ib-IX Complex in Phospholipid Bilayer Nanodiscs†

Rong Yan[1,2], **Xi Mo**[2], **Angel M. Paredes**[3], **Kesheng Dai**[1], **Francois Lanza**[4], **Miguel A. Cruz**[5], and **Renhao Li**[2,6,*]

[1]Ministry of Health Key Laboratory of Thrombosis and Haemostasis, Jiangsu Institute of Hematology, the First Affiliated Hospital of Soochow University, Suzhou, China

[2]Center for Membrane Biology, Department of Biochemistry and Molecular Biology, The University of Texas Health Science Center at Houston, Houston, Texas, USA

[3]Department of Pathology and Laboratory Medicine, The University of Texas Health Science Center at Houston, Houston, Texas, USA

[4]Etablissement de Transfusion Sanguine, INSERM, Unite311, Strasbourg Cedex, France

[5]Thrombosis Research Section, Department of Medicine, Baylor College of Medicine, Houston, Texas, USA

[6]Department of Pediatrics, Division of Hematology/Oncology, Aflac Cancer Center and Blood Disorders Service, Emory University School of Medicine, Atlanta, Georgia, USA

Abstract

Glycoprotein (GP)Ib-IX complex expressed on platelet plasma membrane is involved in thrombosis and hemostasis by initiating platelet adhesion to von Willebrand factor (VWF) exposed at the injured vessel wall. While most of the knowledge for GPIb-IX is obtained from studies on platelets and transfected mammalian cells expressing GPIb-IX, there is not an *in vitro* membrane system that allows systematic analysis of this receptor. The phospholipid bilayer Nanodisc composed of a patch of phospholipid surrounded by membrane scaffold protein is an attractive tool for membrane protein study. We show here that GPIb-IX purified from human platelets has been reconstituted into the Nanodisc. Nanodisc-reconstituted GPIb-IX was able to bind various conformation-sensitive monoclonal antibodies. Furthermore, it bound to VWF in the presence of botrocetin with an apparent K_d of 0.73 ± 0.07 nM. The binding to VWF was inhibited by anti-GPIbα antibodies with epitopes overlapping with the VWF-binding site, but not by anti-GPIbβ monoclonal antibody RAM.1. Finally, Nanodisc-reconstituted GPIb-IX exhibited similar ligand-binding activity as the isolated extracellular domain of GPIbα. In conclusion, GPIb-IX in Nanodiscs adopts native-like conformation and possesses the ability to bind its natural ligands, thus making Nanodisc a suitable *in vitro* platform for further investigation on this hemostatically important receptor complex.

†Supported by NIH grant HL082808.

*Address correspondence to: Renhao Li, Aflac Cancer Center and Blood Disorders Service, 2015 Uppergate Drive, Room 426A, Atlanta, GA 30322. Tel: 404-727-8217; Fax: 404-727-4859; renhao.li@emory.edu.

SUPPORTING INFORMATION

A supplement figure showing the calibration of GPIb and MSP staining in SDS gels is included and available free of charge via the Internet at http://pubs.acs.org.

$watermark-text
$watermark-text
$watermark-text

$watermark-text

$watermark-text

$watermark-text

INTRODUCTION

Cell adhesion receptors not only mediate cell-matrix interactions and cell-cell contacts through ligand binding of their extracellular domains, but also transmit signals into the cell to initiate response to the change in its surroundings. The activity of many adhesion receptors can be regulated by intracellular signals via an apparent inside-out pathway. While the molecular mechanisms underlying the outside-in and inside-out signaling pathways have been the target of numerous studies, most of which are concentrated on the platelet-specific integrin αIIbβ3 (1–3), general principles for the adhesion receptor-mediated transmembrane signaling remain to be elucidated.

The glycoprotein (GP) Ib-IX complex is expressed in the plasma membrane of platelets and plays a critical role in the initiation of thrombosis and hemostasis. This adhesion receptor complex consists of three type I transmembrane protein subunits, GPIbα, GPIbβ and GPIX, with a stoichiometry of 1:2:1 (4, 5). GPIbα connects with two GPIbβ subunits through membrane-proximal disulfide bonds to form a complex called GPIb (5). GPIX is tightly associated with GPIb through noncovalent forces in both extracellular and transmembrane domains (4, 6–8). In the GPIb-IX complex, the N-terminal leucine-rich repeat domain of GPIbα contains the binding site for its physiological ligand VWF (9–11). Upon ligation with the A1 domain of VWF, the GPIb-IX complex transmits inward, through the cytoplasmic tail of GPIbα, an activating signal that leads to activation of integrin αIIbβ3 and eventual platelet aggregation (12, 13). A recent study shows that although mouse platelets expressing a PT-VWD mutation in the N-terminal ligand-binding domain of GPIbα spontaneously binds to VWF as expected, the platelets were surprisingly inactive and failed to respond to agonist treatment, suggesting that the mutant GPIb-IX complex transmits an inhibitory signal into the platelet (14). In addition to mediating outside-in signaling events, GPIb-IX complex undergoes inside-out regulation. For instance, a change in the phosphorylation state of Ser166 in the cytoplasmic domain of GPIbβ can influence VWF binding to the N-terminal domain of GPIbα (15, 16). Moreover, a 27-bp deletion in the macroglycopeptide-coding region of the GPIBA gene has been identified in certain PT-VWD patients (17). The deletion, distal to the ligand-binding domain but proximal to the transmembrane domain of GPIbα, increased the VWF binding function of GPIbα that are heterologously expressed in mammalian cells (17). However, our understanding of the mechanism by which the GPIb-IX complex transmits signals in both directions remains limited, partly due to the difficulty in the characterization of multi-subunit membrane protein complexes as well as the lack of a suitable *in vitro* experimental system for this complex.

Phospholipid bilayer Nanodiscs are novel model membranes derived from nascent discoidal high-density lipoprotein particles (18, 19). One disc contains a patch of phospholipid, which is wrapped by two copies of membrane scaffold protein (MSP) derived from human apolipoprotein A-I (19). Due to the presence of the protein coat MSP, Nanodiscs are soluble and monodisperse and have well-defined diameters, ranging from 9.4 nm to 12 nm depending on the size of MSP (19, 20). Therefore, the membrane proteins placed into the Nanodisc have the “native-like” membrane environment. The exposure of both extracellular and intracellular domains of a membrane protein to the same aqueous environment is particularly amenable to spectroscopic investigations. Indeed Nanodiscs have been adopted in studies of a variety of membrane proteins, including bacteriorhodopsin and G protein-coupled receptors (21–23), bacterial chemoreceptors (24), epidermal growth factor receptor (EGFR) (25) and integrin αIIbβ3 (26).

We have incorporated platelet GPIb-IX complex into the phospholipid bilayer Nanodiscs. The GPIb-IX complex adopts native-like conformation in Nanodiscs and is capable of

$watermark-text

$watermark-text

$watermark-text

binding to VWF with sub-nanomolar binding affinity. An *in vitro* experimental platform has therefore been established for future investigation on the mechanism of the signal transmission through the GPIb-IX complex.

MATERIAL AND METHODS

Reagents and antibodies

POPC was obtained from Avanti Polar Lipids (Alabaster, AL). Monoclonal antibodies against individual subunits of the GPIb-IX complex, including WM23, SZ2, AN51, FM25, AK2 and Gi27, were either obtained from the hybridoma cell line or purchased from Beckman Coulter (Fullerton, CA), Dako (Carpinteria, CA), Millipore (Billerica, MA), AbD Serotec (Raleigh, NC) or Chemicon (Temecula, CA). Mouse and rat IgG and HRP-conjugated secondary antibodies were purchased from Santa Cruz Biotechnology (Santa Cruz, CA). Human VWF and botrocetin were obtained from American Diagnostica Inc. (Greenwich, CT) and Centerchem Inc. (Norwalk, CT), respectively. Bovine pancreas DNase I was from Roche Applied Science (Indianapolis, IN). MSP1D1 plasmid was obtained from Addgene (Cambridge, MA). Monoclonal antibody Ram.1 and the A1A2A3 fragment of VWF were obtained as previously described (27, 28).

Purification of human platelet GPIb-IX complex

Purification of platelet GPIb-IX complex followed published protocols (29, 30) with some modifications. Four units of fresh concentrated PRP were obtained from Gulf Coast Regional Blood Center (Houston, TX), from which platelets were pelleted in the presence of 5 mM EDTA at 1,300 g at room temperature for 10 min and washed once with CGS buffer (120 mM NaCl, 30 mM D-glucose, 12.9 mM trisodium citrate, pH 6.5) containing 5 mM EDTA. Pelleted platelets were resuspended in buffer A (20 mM Tris·HCl, 150 mM NaCl, 10 mM EDTA, pH 7.4) with 200 mM sucrose, 1:50 (v/v) dilution of protease inhibitor cocktail (Sigma, St Louis, MO) and 1 mM PMSF (Amresco, Solon, OH) and sonicated with a Branson Sonifier 250 (Branson, Danbury, CT) until the suspension became clear. Platelet membrane portion was extracted from the lysate by centrifugation at 180,000 g at 4 °C for 1 hour and then dissolved in ice-cold buffer A containing 1% Triton X-100, 5 mM N-ethylmaleimide (Sigma), 1:50 dilution of protease inhibitor cocktail and 1 mM PMSF at 4 °C for 2 hours. Triton X-100-soluble fraction was isolated by centrifugation at 180,000 g at 4 °C for 3 hours to remove the cytoskeleton.

The soluble fraction was incubated with 2 mg/ml DNase I on ice for 1.5 hours to depolymerize any remaining actin filaments and then applied to a wheat germ agglutinin (WGA) column (Calbiochem, San Diego, CA). The column was washed thoroughly by buffer B (20 mM Tris·HCl, 150 mM NaCl, 1 mM EDTA, 0.1% Triton X-100, pH 7.4) and the bound proteins eluted by buffer B containing 2.5% N-acetyl-D-glucosamine (Sigma). The eluent was further purified with anion exchange chromatography (Resource Q column, GE healthcare, Piscataway, NJ) using a linear gradient of 0.15–1 M NaCl in 20 mM Tris·HCl, 1 mM EDTA, 0.1% Triton X-100, pH 7.4. The eluted GPIb-IX complex was concentrated and changed to buffer B using Amicon Ultra 15 ml filters with 10-kDa MWCO (Millipore) before being stored at −80 °C. The concentration of GPIb-IX was determined using BCA protein assay kit (Pierce Biotechnology, Rockford, IL).

Purification of platelet glycocalicin

Glycocalicin, also known as the soluble extracellular domain of GPIbα, was isolated from human platelets by a variation of an earlier method (31). Briefly, platelets were pelleted from 3 units of fresh PRP at 1,300 g for 10 min at room temperature. The pelleted platelets were washed once with CGS buffer, resuspended in 40 ml TBS buffer (20 mM Tris·HCl,

100 mM NaCl, pH 7.4) containing 2 mM $CaCl_2$ and sonicated to lyse the cells. The mixture was then incubated at 37 °C for 1 h to allow the proteolytic cleavage of GPIbα to generate glycocalicin. 1 mM PMSF and 5 mM EDTA were added to quench further proteolysis after the incubation. After ultracentrifugation at 80,000 g and 4 °C for 1 h to remove cell components, the glycocalicin-containing supernatant was applied to WGA column. After washing with TBS buffer, the bound proteins were eluted with the elution buffer (20 mM Tris·HCl, 2.5% N-actyl-D-glucosamine, pH 7.4). The eluent was further loaded to Resource Q column with a linear gradient of 0–1 M NaCl in 20 mM Tris·HCl, pH 7.4 over 40 ml. Glycocalicin was further purified through a Superose 6 10/300 GL gel filtration column (GE healthcare).

Reconstitution of GPIb-IX complex in Nanodiscs

MSP1D1 was expressed in *E. coli* BL21(DE3) cells and purified by Ni-affinity chromatography following the published protocol (18). POPC dissolved in chloroform was dried in a glass vial by a gentle argon stream to a thin film and placed under vacuum overnight to remove residual solvent. The dried lipid was hydrated with the hydration buffer (20 mM Tris·HCl, 100 mM NaCl, 100 mM sodium cholate, 0.01% NaN_3, pH 7.4) to a final concentration of 50 mM.

Empty Nanodiscs and GPIb-IX-containing Nanodiscs (GPIb-IX/ND) were assembled according to the published protocols (25, 32). Briefly, 300 μL assembly reaction containing 1 mM POPC, 25 μM MSP1D1, 16 mM sodium cholate without or with 1 μM GPIb-IX was incubated at room temperature for 45 min and then placed on ice for 1 hour. Nanodisc assembly was initiated with the addition of 0.15 g (empty Nanodiscs) or 0.24 g (GPIb-IX/ND) damp Bio-beads SM-2 (Bio-Rad, Richmond, CA) and the reaction complex was gently rocked at 4 °C for 16 hours. After assembly, the Bio-beads were removed by centrifugation at 10,000 g for 1 min and the supernatant applied to a Superose 6 10/300 GL column (GE healthcare) calibrated by molecular weight standards (Bio-Rad) to analyze the mixture and to purify assembled Nanodiscs.

ELISA

Nanodiscs (~4 μg/ml) or 1% BSA (R&D system, Minneapolis, MN) was immobilized onto microtiter plate at 4°C overnight and the wells were blocked with 1% BSA in PBS. To probe the conformation of GPIb-IX, conformation-sensitive monoclonal antibodies against various components of GPIb-IX were added to Nanodiscs- or BSA-coated wells followed by either HRP-conjugated goat anti-mouse IgG or goat anti-rat IgG. To measure binding of VWF, various concentrations of VWF with 0.2 U/ml botrocetin was added, followed by rabbit anti-VWF antibody (2 μg/ml) and HRP-conjugated goat anti-rabbit IgG (1:5000). The incubation was carried out at room temperature for 1 h unless specifically stated and wells were washed 4 times with PBS between every two steps. After incubation of antibodies and standard washing, substrate tetramethylbenzidine (R&D systems) was added to each well and incubated for 20 min. The reaction was stopped by addition of 25 μL 1M H_2SO_4 to each well and the plate was read at 450 nm (with wavelength correction at 570 nm) in a Dynex MRX ELISA plate reader (Dynex technologies, Chanilly, VA).

To compare the ligand-binding function of GPIb-IX versus glycocalicin, 4 μg/ml WM23 in PBS was first immobilized in the microtiter wells at 4°C overnight. After blocking with 1% BSA in PBS, GPIb-IX/ND, glycocalicin as well as empty Nanodiscs and 4 μg/ml BSA were added to the wells. After capture, full length VWF or A1A2A3 domains with 0.2 U/ml botrocetin were incubated and the binding was detected with rabbit anti-VWF antibody and HRP-conjugated goat anti-rabbit antibody. To compare the efficiency of capturing, WM23 $F(ab')_2$ fragment was generated using mouse IgG $F(ab')_2$ fragment preparation kit (Pierce

$watermark-text $watermark-text $watermark-text

$watermark-text

$watermark-text

$watermark-text

Biotechnology) and used to coat the wells. Anti-GPIbα monoclonal antibody and HRP-conjugated goat anti-mouse IgG Fc (Pierce Biotechnology) were used to detect captured GPIb-IX/ND and glycocalicin. After subtracting the background signal, the binding curve was fitted to equation

$$Y=B_{max} * x/(K_d+x)$$

where Y is the specific binding, x the ligand concentration, B_{max} the binding maximum and K_d the equilibrium dissociation constant.

Electron microscopy of Nanodiscs

Purified GPIb-IX/ND (~10 μg/ml in 20 mM Tris·HCl, pH 7.4) was applied to a copper EM grid containing a carbon film support. The specimen was stained with 0.7% uranyl acetate. Images were taken on a model JEM-1200 EX transmission electron microscope (JEOL, Peabody, MA) at a magnification of 40,000 and recorded on a TVIPS F215 2k x 2k CCD camera (TVIPS, Gauting, Germany).

RESULTS

Assembly of platelet GPIb-IX complex into phospholipid Nanodiscs

The GPIb-IX GPIb-IX complex was purified from human platelet concentrates. Figure 1A shows the SDS-PAGE profile of purified GPIb-IX. Under non-reducing conditions, GPIb and GPIX bands were present in the SDS gel, constituting over 95% of the detectable protein. Under reducing conditions, GPIb dissociates into GPIbα and GPIbβ subunits (4, 5). To determine the size of the complex before being assembled into Nanodiscs, purified GPIb-IX in the Triton X-100-containing buffer was analyzed by gel filtration chromatography (Fig. 1B). Partly due to the elongated shape of GPIbα (33), the complex was eluted with a Stokes diameter of approximately 24 nm.

Empty Nanodiscs were first assembled using POPC and MSP1D1. The molar ratio of POPC:MSP1D1 was optimized to minimize protein aggregation and maximize Nanodisc assembly. As shown in Figure 2A, empty Nanodiscs were eluted with a Stokes diameter of approximately 9.5 nm from the gel filtration column, consistent with a Stokes diameter of 9.5 nm for Nanodiscs comprising of MSP1D1 and DMPC (20) and 9.6 nm for those of MSP1D1 and egg PC (25). Visualization of MSP1D1 in a SDS gel shown in Figure 2B and TEM image of empty Nanodiscs in Figure 2C confirmed the success of assembly.

To assemble the GPIb-IX complex into Nanodiscs, GPIb-IX-solubilized in 0.1% Triton X-100 was mixed with excess MSP1D1 and POPC so that at most one copy of the complex was reconstituted into a Nanodisc. After removal of detergent by Bio-beads, the mixture was analyzed by gel filtration chromatography. In addition to the peak of empty Nanodiscs, another well-separated peak with an apparent Stokes diameter of approximately 27 nm was observed (Fig. 2D). This peak contained GPIb-IX-embedded Nanodiscs (GPIb-IX/ND), since GPIb and MSP1D1 were co-eluted from the column (Fig. 2E). The presence of both GPIbα and GPIX in the discs was further confirmed by ELISA (Fig. 3). The Stokes diameter of GPIb-IX/ND is slightly larger than that of GPIb-IX in Triton X-100-containing buffer, consistent with the expectation that a Nanodisc is larger than a detergent micelle. The TEM image shows the disc-shape density, further confirming the success of assembly (Fig. 2F). As a negative control, the GPIb-IX complex was mixed with POPC but without MSP, and it was eluted at void volume (Fig. 2D), indicating that the complex was reconstituted into POPC lipid vesicles or it formed large aggregates during the process.

$watermark-text

$watermark-text

$watermark-text

To determine the stoichiometry of GPIb-IX-containing Nanodiscs, intensities of GPIb and MSP1D1 protein bands in Figure 2E were compared and the molar ratio of GPIb to MSP1D1 was calculated to approximately 0.4:1 based on calibration of the difference between the Coomassie blue staining efficiency of GPIb and MSP1D1 in SDS gels (Figure S1). Since there are two copies of MSP1D1 per disc, our results suggested that only one copy of GPIb-IX complex was incorporated into a Nanodisc.

VWF-binding function of GPIb-IX reconstituted in Nanodiscs

To evaluate the quality of GPIb-IX reconstituted in Nanodiscs, we first probed the conformation of GPIbα and GPIX using conformation-sensitive monoclonal antibodies. SZ2, AN51 and AK2 recognize distinct three-dimensional epitopes in or around the N-terminal ligand-binding domain of GPIbα (34, 35), whereas FMC25 recognizes only the well-folded GPIX ectodomain (30). GPIb-IX/ND, empty Nanodiscs or BSA was directly coated to microtiter wells and antibody binding detected by ELISA with HRP-conjugated secondary antibody. As shown in Figure 3, all the monoclonal antibodies tested bound to wells coated with GPIb-IX/ND but not to those with empty Nanodisc or BSA, indicating that GPIb-IX reconstituted in Nanodiscs adopts native-like conformation. Moreover, the conformation of GPIb-IX/ND is stable as it retains binding to conformation-sensitive antibodies after being stored at 4 °C for two weeks (data not shown).

Next we determined the binding affinity of VWF to GPIb-IX/ND in the presence of botrocetin, which mediates the interaction between GPIbα and VWF under static conditions (36). Since it is more difficult to accurately measure the concentration of GPIb-IX/ND than that of VWF, GPIb-IX/ND was immobilized in the ELISA assay and the amount of bound VWF in the microtiter well was measured using anti-VWF antibody. Figure 4A shows that VWF bound to GPIb-IX/ND in a concentration-dependent and saturable manner, with apparent dissociation constant of 0.73 ± 0.07 nm if the molar concentration of VWF was calculated with a molecular weight of 250 kDa. The measured dissociation constant is the same as that observed from fixed human platelets (data not shown) and comparable with those in previous reports (37, 38). The effects of antibodies against each subunit of GPIb-IX complex on VWF binding were also tested. AK2, targeting the ligand-binding domain of GPIbα (34), abolished botrocetin-induced VWF binding, indicating that the binding is specific to GPIbα. As expected, FMC25, targeting the GPIX extracellular domain, or Gi27, targeting the GPIbβ cytoplasmic domain, had no effect (Fig. 4B). Overall, these results showed that GPIb-IX retains its normal ligand-binding function when reconstituted in Nanodiscs.

The effect of RAM.1 on VWF binding to GPIb-IX in Nanodiscs

Although the binding site for VWF is located on the N-terminus of GPIbα, GPIbβ has been shown to regulate the ligand-binding function of GPIbα, either through their cytoplasmic tails (15, 16) or the membrane-proximal disulfide bonds (39). RAM.1, a rat monoclonal antibody that recognizes the extracellular part (Cys68-Cys93) of GPIbβ, hampers botrocetin-induced binding of platelets or GPIb-IX-transfected cells to VWF as well as their adhesion to VWF under flow conditions (27, 40). We tested here whether RAM.1 can hamper the association of GPIb-IX/ND with VWF *in vitro*. As shown in Figure 5A, RAM.1 bound to GPIb-IX/ND, but not to empty Nanodiscs or BSA, that were immobilized in microtiter wells. However, after 10 μg/ml Rat IgG or RAM.1 was pre-incubated with immobilized GPIb-IX/ND, no significant difference in botrocetin-mediated VWF binding was observed (Fig. 5B). Similar results were observed when a higher concentration of RAM.1 was used in pre-incubation, or when GPIb-IX/ND was captured by WM23 instead of being coated directly onto microtiter wells, or when recombinant A1A2A3 tri-domains of VWF was used for binding. Thus, these results suggest that the effect of RAM.1 on VWF binding observed

in platelets or GPIb-IX-transfected cells may not be due to a direct interference with the VWF-GPIbα interaction and thus is unlikely to restrict to the extracellular domain of GPIbβ.

Comparison of ligand binding between GPIb-IX/ND and glycocalicin

To further investigate the role of GPIbβ in the ligand-binding function of GPIbα, binding of full-length VWF or A1A2A3 tri-domains to GPIb-IX/ND in the presence of botrocetin were compared to those to glycocalicin by ELISA. Since glycocalicin could not be recognized by AN51 when it was directly coated to microtiter wells, WM23, a mouse monoclonal antibody targeting the macroglycopeptide portion of GPIbα, was used to capture GPIb-IX/ND and glycocalicin in microtiter wells. Although ELISA results showed that apparent dissociation constants obtained for interaction with full-length VWF or A1A2A3 tri-domains were indistinguishable between GPIb-IX/ND and glycocalicin, the amount of bound VWF or A1A2A3 were different for GPIb-IX/ND and glycocalicin (Fig. 6A, B). To explain this difference, SZ2, a monoclonal antibody targeting the N-terminal domain of GPIbα, was used to detect the amount of GPIb-IX/ND and glycocalicin immobilized by WM23 $F(ab')_2$ fragment in microtiter wells. As shown in Figure 6C, significantly more GPIb-IX/ND was present in the well than glycocalicin although the same amount of WM23 $F(ab')_2$ fragment was used for immobilization. Moreover, the difference in WM23's capturing abilities between GPIb-IX/ND and glycocalicin matches the difference in bound A1A2A3 tri-domains in ELISA assays, indicating that the apparent lower binding of A1A2A3 to glycocalicin is due to the lower capture efficiency of glycocalicin by WM23 (Fig. 6B). Since full-length VWF is multimeric, the amount of bound VWF may not be simply correlated with that of captured receptor. Thus, there appeared to be little difference in the ligand-binding function between GPIb-IX reconstituted in Nanodiscs and glycocalicin in the presence of botrocetin.

DISCUSSION

Comparing to detergent micelles, Nanodiscs provide membrane proteins with a real phospholipid bilayer environment that mimics the cell membrane. Phosphotidylcholine, the most abundant phospholipid in cell membranes, was used in this study to construct the Nanodisc. Comparing to phospholipid vesicles, Nanodiscs also offer several advantages (19). One of the advantages is the simultaneous access to both extracellular and cytoplasmic domains of the membrane receptor embedded in Nanodiscs. This is particularly useful for mechanistic studies on receptor-mediated signal transduction across the membrane (24, 26). Thus, reconstitution of the functional GPIb-IX complex into phospholipid Nanodiscs will provide a useful platform for mechanistic investigations on GPIb-IX-mediated transmembrane signaling events.

In this study we have reconstituted purified GPIb-IX complex into phospholipid Nanodiscs and shown that the GPIb-IX complex is functional in this novel model membrane. Incorporation of the GPIb-IX complex into Nanodiscs was confirmed by three lines of evidence. First, MSP1D1 co-eluted with GPIb from the gel filtration column after assembly. Co-elution of 25-kDa MSP1D1 with 220-kDa GPIb-IX indicates that they are bound together and eluted as a complex. Second, GPIb-IX/ND eluted at a slightly larger Stokes diameter than GPIb-IX dissolved in the Triton X-100-containing buffer. The average molecular weight of a Triton X-100 micelle is 80 kDa (41). Assuming that there are 160 molecules of POPC in each Nanodisc, the molecular weight of one empty disc is 170 kDa (20). The larger molecular weight of a disc compared to a detergent micelle would explain the slightly larger Stokes diameter of GPIb-IX/ND. Similar difference was also observed for EGFR reconstituted in Nanodiscs versus that dissolved in the Triton X-100-containing

$watermark-text $watermark-text $watermark-text

$watermark-text

$watermark-text

$watermark-text

buffer (26). Finally, the negative-stain TEM image of GPIb-IX/ND showed the disc-shape density, consistent with previous reports (42).

Reconstituted in the Nanodisc, the GPIb-IX complex adopts the native conformation as it is able to bind all the conformation-sensitive antibodies tested in this study. GPIb-IX in Nanodiscs is stable for at least two weeks (data not shown). Moreover, it shows native-like ligand-binding properties, having exhibited the same binding affinity for VWF in the presence of botrocetin as in previous reports (37, 38). The binding affinity measured in this study is also comparable to those previously reported for the binding of N-terminal fragment of GPIbα to VWF in the presence of botrocetin (11, 43).

GPIbβ plays a central role in assembly of the GPIb-IX complex. It interacts with GPIbα through a disulfide bond near the membrane as well as interactions between their transmembrane domain (5, 44, 45). There is also cross-talk between the cytoplasmic tails of these two subunits through the association with 14-3-3ζ (15). Relatedly, binding of antibody RAM.1 to the GPIbβ extracellular domain leads to the alteration of the cytoplasmic tails of GPIb and at the same time hampers the ligand-binding ability of the extracellular domain of GPIbα (40). The molecular mechanism underlying GPIbβ modulation of VWF-binding function of GPIbα is not clear. One possible mechanism may be that the GPIbβ extracellular domain, or in the presence of RAM.1, directly participates in an interaction with VWF and thus directly modulates the GPIbα-VWF interaction. To test this possibility, we compared binding of VWF to glycocalicin versus GPIb-IX/ND. Consistent with a previous study (38), although glycocalicin and GPIb-IX/ND for some reason exhibit different immobilization efficiency by WM23, little difference in binding affinity was observed (Fig. 6). Furthermore, while RAM.1 exhibited specific binding to GPIb-IX/ND, it did not have any detectable effect on VWF association to GPIb-IX/ND in the presence of botrocetin (Fig. 5). These results indicate that the GPIbβ extracellular domain may not directly participate in the interaction with VWF or modulate the GPIbα-VWF interaction, and that the observed RAM.1 effects on VWF-binding by platelets and GPIb-IX-expressing cells may require other factors inside the cell. One possible scenario is that RAM.1 binding to the GPIbβ extracellular domain may transmit a signal into the platelet, through perhaps 14-3-3ζ association with cytoplasmic domains of GPIb-IX (15, 16, 46–48), and influence the surface distribution and/or the overall binding activity of GPIb-IX. Further investigation will be needed to elucidate the apparent trans-subunit effects of RAM.1 on GPIb-IX function and signaling.

Supplementary Material

Refer to Web version on PubMed Central for supplementary material.

Acknowledgments

We thank Ms. Katie Sowa and Limei H. Jones for technical assistance.

Abbreviations

PT-VWD	platelet-type von Willebrand disease
POPC	1-palmitoyl-2-oleoyl-*sn*-glycero-3-phosphocholine
HRP	Horseradish Peroxidase
PRP	platelet rich plasma
PMSF	phenylmethylsulfonyl fluoride

$watermark-text

$watermark-text

$watermark-text

ELISA	Enzyme-linked immunosorbent assay
BSA	bovine serum albumin
TEM	transmission electron microscopy

References

1. Takagi J, Petre BM, Walz T, Springer TA. Global conformational rearrangements in integrin extracellular domains in outside-in and inside-out signaling. Cell. 2002; 110:599–611. [PubMed: 12230977]
2. Vinogradova O, Velyvis A, Velyviene A, Hu B, Haas TA, Plow EF, Qin J. A structural mechanism of integrin αIIbβ3 "inside-out" activation as regulated by its cytoplasmic face. Cell. 2002; 110:587–597. [PubMed: 12230976]
3. O'Toole TE, Mandelman D, Forsyth J, Shattil SJ, Plow EF, Ginsberg MH. Modulation of the affinity of integrin αIIbβ3 (GPIIb-IIIa) by the cytoplasmic domain of αIIb. Science. 1991; 254:845–847. [PubMed: 1948065]
4. Du X, Beutler L, Ruan C, Castaldi PA, Berndt MC. Glycoprotein Ib and glycoprotein IX are fully complexed in the intact platelet membrane. Blood. 1987; 69:1524–1527. [PubMed: 2436691]
5. Luo S-Z, Mo X, Afshar-Kharghan V, Srinivasan S, Lopez JA, Li R. Glycoprotein Ibα forms disulfide bonds with 2 glycoprotein Ibβ subunits in the resting platelet. Blood. 2007; 109:603–609. [PubMed: 17008541]
6. Luo SZ, Mo X, López JA, Li R. Role of the transmembrane domain of glycoprotein IX in assembly of the glycoprotein Ib-IX complex. J Thromb Haemost. 2007; 5:2494–2502. [PubMed: 17922811]
7. Mo X, Nguyen NX, McEwan PA, Zheng X, Lopez JA, Emsley J, Li R. Binding of platelet glycoprotein Ibβ through the convex surface of leucine-rich repeats domain of glycoprotein IX. J Thromb Haemost. 2009; 7:1533–1540. [PubMed: 19566547]
8. McEwan PA, Yang W, Carr KH, Mo X, Zheng X, Li R, Emsley J. Quaternary organization of GPIb-IX complex and insights into Bernard-Soulier syndrome revealed by the structures of GPIbβ and a GPIbβ/GPIX chimera. Blood. 2011 Epub ahead of print.
9. Huizinga EG, Tsuji S, Romijn RA, Schiphorst ME, de Groot PG, Sixma JJ, Gros P. Structures of glycoprotein Ibα and its complex with von Willebrand factor A1 domain. Science. 2002; 297:1176–1179. [PubMed: 12183630]
10. Cauwenberghs N, Vanhoorelbeke K, Vauterin S, Deckmyn H. Structural determinants within platelet glycoprotein Ibα involved in its binding to von Willebrand factor. Platelets. 2000; 11:373–378. [PubMed: 11132103]
11. Miura S, Li CQ, Cao Z, Wang H, Wardell MR, Sadler JE. Interaction of von Willebrand factor domain A1 with platelet glycoprotein Ibα-(1–289), Slow intrinsic binding kinetics mediate rapid platelet adhesion. J Biol Chem. 2000; 275:7539–7546. [PubMed: 10713059]
12. Kroll MH, Harris TS, Moake JL, Handin RI, Schafer AI. von Willebrand factor binding to platelet GpIb initiates signals for platelet activation. J Clin Invest. 1991; 88:1568–1573. [PubMed: 1939645]
13. Savage B, Shattil SJ, Ruggeri ZM. Modulation of platelet function through adhesion receptors. A dual role for glycoprotein IIb-IIIa (integrin αIIbβ3) mediated by fibrinogen and glycoprotein Ib-von Willebrand factor. J Biol Chem. 1992; 267:11300–11306. [PubMed: 1597464]
14. Guerrero JA, Kyei M, Russell S, Liu J, Gartner TK, Storrie B, Ware J. Visualizing the von Willebrand factor/glycoprotein Ib-IX axis with a platelet-type von Willebrand disease mutation. Blood. 2009; 114:5541–5546. [PubMed: 19808696]
15. Dai K, Bodnar R, Berndt MC, Du X. A critical role for 14-3-3ζ protein in regulating the VWF binding function of platelet glycoprotein Ib-IX and its therapeutic implications. Blood. 2005; 106:1975–1981. [PubMed: 15941906]
16. Bodnar RJ, Xi X, Li Z, Berndt MC, Du X. Regulation of glycoprotein Ib-IX-von Willebrand factor interaction by cAMP-dependent protein kinase-mediated phosphorylation at Ser 166 of glycoprotein Ibβ. J Biol Chem. 2002; 277:47080–47087. [PubMed: 12361948]

$watermark-text

$watermark-text

$watermark-text

17. Othman M, Notley C, Lavender FL, White H, Byrne CD, Lillicrap D, O'Shaughnessy DF. Identification and functional characterization of a novel 27-bp deletion in the macroglycopeptide-coding region of the GPIbα gene resulting in platelet-type von Willebrand disease. Blood. 2005; 105:4330–4336. [PubMed: 15705799]
18. Bayburt TH, Grinkova YV, Sligar SG. self-assembly of discoidal phospholipid bilayer nanoparticles with membrane scaffold proteins. Nano Let. 2002; 2:853–856.
19. Nath A, Atkins WM, Sligar SG. Applications of phospholipid bilayer nanodiscs in the study of membranes and membrane proteins. Biochemistry. 2007; 46:2059–2069. [PubMed: 17263563]
20. Denisov IG, Grinkova YV, Lazarides AA, Sligar SG. Directed self-assembly of monodisperse phospholipid bilayer Nanodiscs with controlled size. J Am Chem Soc. 2004; 126:3477–3487. [PubMed: 15025475]
21. Bayburt TH, Grinkova YV, Sligar SG. Assembly of single bacteriorhodopsin trimers in bilayer nanodiscs. Arch Biochem Biophys. 2006; 450:215–222. [PubMed: 16620766]
22. Bayburt TH, Sligar SG. Self-assembly of single integral membrane proteins into soluble nanoscale phospholipid bilayers. Protein Sci. 2003; 12:2476–2481. [PubMed: 14573860]
23. Whorton MR, Bokoch MP, Rasmussen SG, Huang B, Zare RN, Kobilka B, Sunahara RK. A monomeric G protein-coupled receptor isolated in a high-density lipoprotein particle efficiently activates its G protein. Proc Natl Acad Sci USA. 2007; 104:7682–7687. [PubMed: 17452637]
24. Boldog T, Grimme S, Li M, Sligar SG, Hazelbauer GL. Nanodiscs separate chemoreceptor oligomeric states and reveal their signaling properties. Proc Natl Acad Sci USA. 2006; 103:11509–11514. [PubMed: 16864771]
25. Mi LZ, Grey MJ, Nishida N, Walz T, Lu C, Springer TA. Functional and structural stability of the epidermal growth factor receptor in detergent micelles and phospholipid nanodiscs. Biochemistry. 2008; 47:10314–10323. [PubMed: 18771282]
26. Ye F, Hu G, Taylor D, Ratnikov B, Bobkov AA, McLean MA, Sligar SG, Taylor KA, Ginsberg MH. Recreation of the terminal events in physiological integrin activation. J Cell Biol. 2010; 188:157–173. [PubMed: 20048261]
27. Perrault C, Moog S, Rubinstein E, Santer M, Baas MJ, de la Salle C, Ravanat C, Dambach J, Freund M, Santoso S, Cazenave JP, Lanza F. A novel monoclonal antibody against the extracellular domain of GPIbβ modulates vWF mediated platelet adhesion. Thromb Haemost. 2001; 86:1238–1248. [PubMed: 11816713]
28. Auton M, Cruz MA, Moake J. Conformational stability and domain unfolding of the Von Willebrand factor A domains. J Mol Biol. 2007; 366:986–1000. [PubMed: 17187823]
29. Fox JE. Linkage of a membrane skeleton to integral membrane glycoproteins in human platelets. Identification of one of the glycoproteins as glycoprotein Ib. J Clin Invest. 1985; 76:1673–1683. [PubMed: 2932470]
30. Berndt MC, Gregory C, Kabral A, Zola H, Fournier D, Castaldi PA. Purification and preliminary characterization of the glycoprotein Ib complex in the human platelet membrane. Eur J Biochem. 1985; 151:637–649. [PubMed: 3161731]
31. Hess D, Schaller J, Rickli EE, Clemetson KJ. Identification of the disulphide bonds in human platelet glycocalicin. Eur J Biochem. 1991; 199:389–393. [PubMed: 2070794]
32. Denisov IG, Baas BJ, Grinkova YV, Sligar SG. Cooperativity in cytochrome P450 3A4: linkages in substrate binding, spin state, uncoupling, and product formation. J Biol Chem. 2007; 282:7066–7076. [PubMed: 17213193]
33. Fox JE, Aggerbeck LP, Berndt MC. Structure of the glycoprotein Ib-IX complex from platelet membranes. J Biol Chem. 1988; 263:4882–4890. [PubMed: 3280570]
34. Shen Y, Romo GM, Dong JF, Schade A, McIntire LV, Kenny D, Whisstock JC, Berndt MC, Lopez JA, Andrews RK. Requirement of leucine-rich repeats of glycoprotein (GP) Ibalpha for shear-dependent and static binding of von Willebrand factor to the platelet membrane GP Ib-IX-V complex. Blood. 2000; 95:903–910. [PubMed: 10648402]
35. Ward CM, Andrews RK, Smith AI, Berndt MC. Mocarhagin, a novel cobra venom metalloproteinase, cleaves the platelet von Willebrand factor receptor glycoprotein Ibα, Identification of the sulfated tyrosine/anionic sequence Tyr-276-Glu-282 of glycoprotein Ibα as a

binding site for von Willebrand factor and α-thrombin. Biochemistry. 1996; 35:4929–4938. [PubMed: 8664285]

36. Andrews RK, Booth WJ, Gorman JJ, Castaldi PA, Berndt MC. Purification of botrocetin from Bothrops jararaca venom. Analysis of the botrocetin-mediated interaction between von Willebrand factor and the human platelet membrane glycoprotein Ib-IX complex. Biochemistry. 1989; 28:8317–8326. [PubMed: 2557900]
37. Hoylaerts MF, Nuyts K, Peerlinck K, Deckmyn H, Vermylen J. Promotion of binding of von Willebrand factor to platelet glycoprotein Ib by dimers of ristocetin. Biochem J. 1995; 306:453–463. [PubMed: 7887899]
38. Meyer S, Kresbach G, Haring P, Schumpp-Vonach B, Clemetson KJ, Hadvary P, Steiner B. Expression and characterization of functionally active fragments of the platelet glycoprotein (GP) Ib-IX complex in mammalian cells. Incorporation of GP Ibα into the cell surface membrane. J Biol Chem. 1993; 268:20555–20562. [PubMed: 8376410]
39. Mo X, Luo SZ, Munday AD, Sun W, Berndt MC, Lopez JA, Dong J-f, Li R. The membrane-proximal intermolecular disulfide bonds in glycoprotein Ib influence receptor binding to von Willebrand factor. J Thromb Haemost. 2008; 6:1789–1795. [PubMed: 18647229]
40. Perrault C, Mangin P, Santer M, Baas MJ, Moog S, Cranmer SL, Pikovski I, Williamson D, Jackson SP, Cazenave JP, Lanza F. Role of the intracellular domains of GPIb in controlling the adhesive properties of the platelet GPIb/V/IX complex. Blood. 2003; 101:3477–3484. [PubMed: 12522011]
41. Biaselle CJ, Millar DB. Studies on Triton X-100 detergent micelles. Biophys Chem. 1975; 3:355–361. [PubMed: 1191737]
42. Tsukamoto H, Sinha A, DeWitt M, Farrens DL. Monomeric rhodopsin is the minimal functional unit required for arrestin binding. J Mol Biol. 2010; 399:501–511. [PubMed: 20417217]
43. Murata M, Ware J, Ruggeri ZM. Site-directed mutagenesis of a soluble recombinant fragment of platelet glycoprotein Ibα demonstrating negatively charged residues involved in von Willebrand factor binding. J Biol Chem. 1991; 266:15474–15480. [PubMed: 1651333]
44. Mo X, Lu N, Padilla A, López JA, Li R. The transmembrane domain of glycoprotein Ibβ is critical to efficient expression of glycoprotein Ib-IX complex in the plasma membrane. J Biol Chem. 2006; 281:23050–23059. [PubMed: 16757483]
45. Luo SZ, Li R. Specific heteromeric association of four transmembrane peptides derived from platelet glycoprotein Ib-IX complex. J Mol Biol. 2008; 382:448–457. [PubMed: 18674540]
46. Calverley DC, Kavanagh TJ, Roth GJ. Human signaling protein 14-3-3ζ interacts with platelet glycoprotein Ib subunits Ibα and Ibβ. Blood. 1998; 91:1295–1303. [PubMed: 9454760]
47. Mangin P, David T, Lavaud V, Cranmer SL, Pikovski I, Jackson SP, Berndt MC, Cazenave JP, Gachet C, Lanza F. Identification of a novel 14-3-3ζ binding site within the cytoplasmic tail of platelet glycoprotein Ibα. Blood. 2004; 104:420–427. [PubMed: 15054037]
48. David T, Ohlmann P, Eckly A, Moog S, Cazenave JP, Gachet C, Lanza F. Inhibition of adhesive and signaling functions of the platelet GPIb-V-IX complex by a cell penetrating GPIbα peptide. J Thromb Haemost. 2006; 4:2645–2655. [PubMed: 17100656]

$watermark-text
$watermark-text
$watermark-text

$watermark-text
$watermark-text
$watermark-text

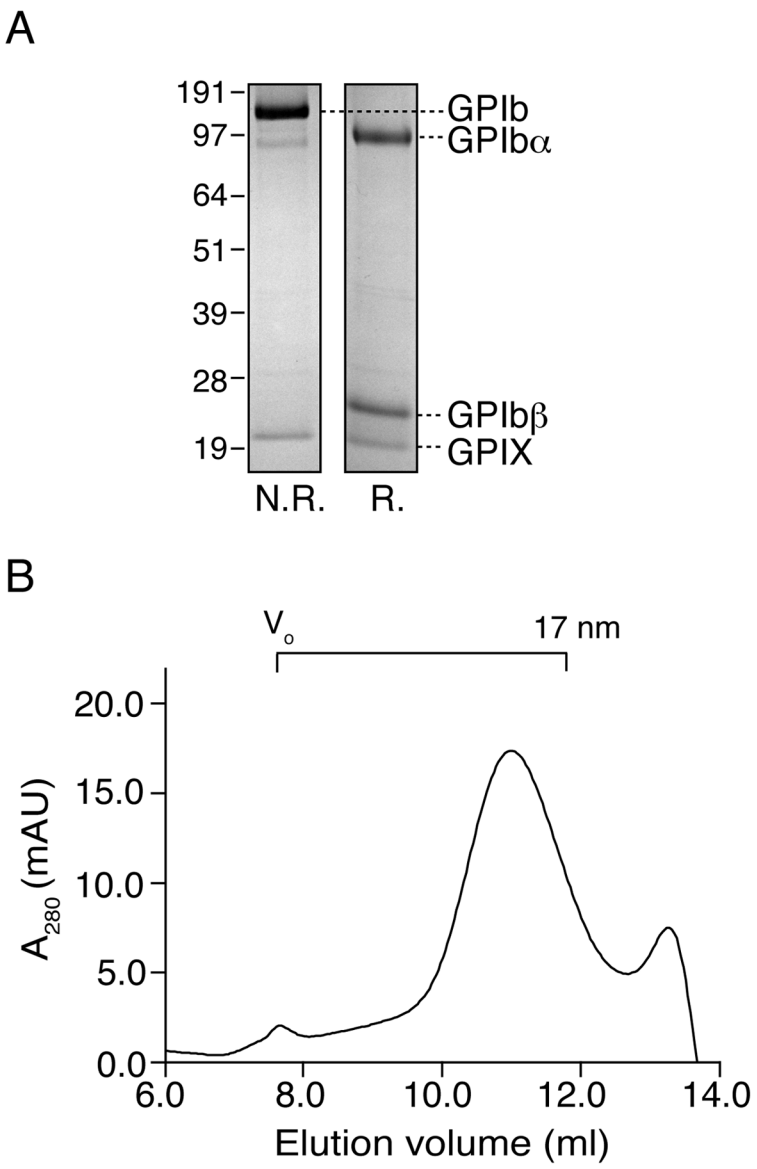

Figure 1. Characterization of purified GPIb-IX complex in Triton X-100

(A) GPIb-IX complex was purified from human platelets and solubilized in 0.1% Triton X-100-containing buffer. The complex was resolved in a 10% SDS gel under both non-reducing (N.R.) and reducing (R.) conditions and detected by Coomassie blue staining. (B) The purified GPIb-IX complex was applied to a gel filtration column Superose 6 equilibrated with 0.1% Triton X-100-containing buffer. Protein elution was monitored by absorbance at 280 nm (A_{280}). The calibrated Stokes diameter scale and void volume for this column are shown at the top.

$watermark-text
$watermark-text
$watermark-text

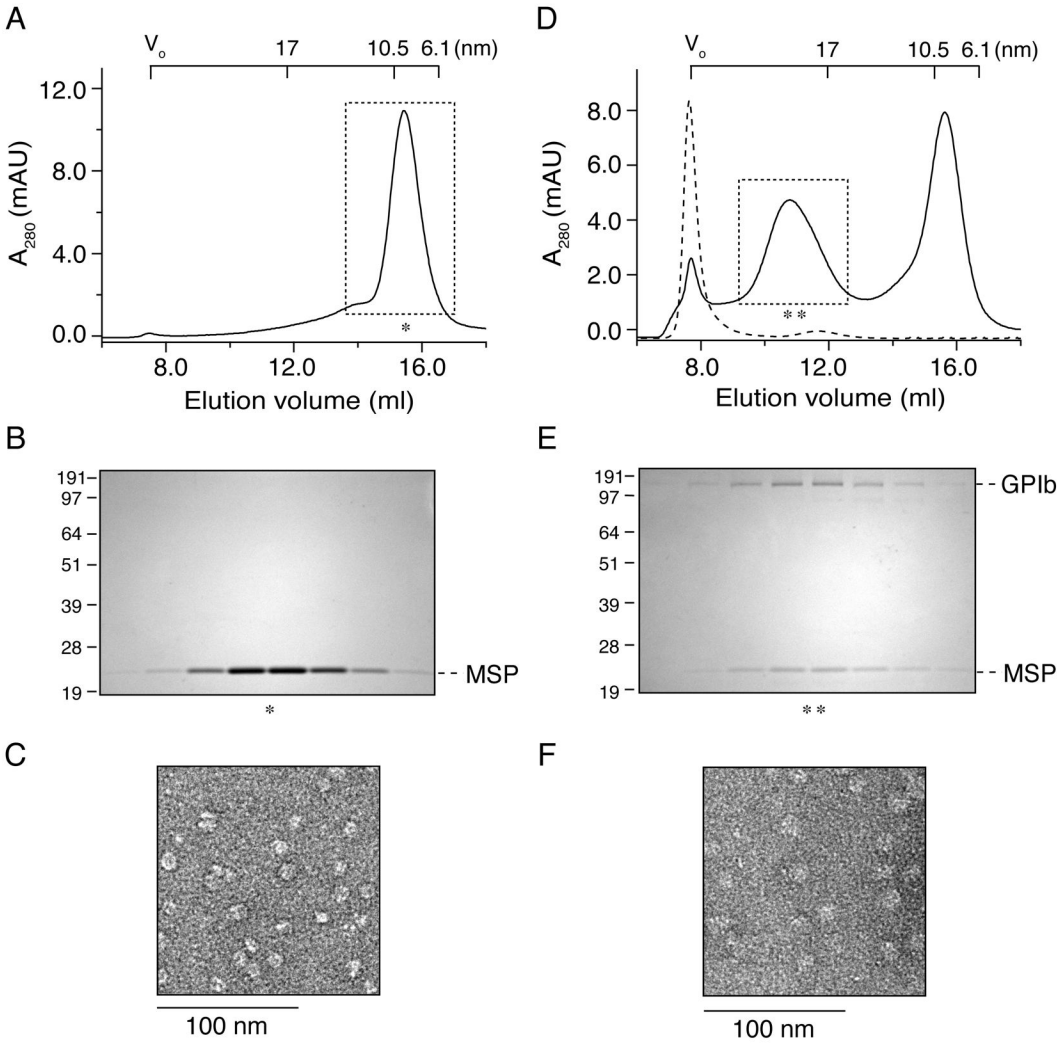

Figure 2. Assembly of purified platelet GPIb-IX complex into phospholipid bilayer Nanodiscs

(A) Empty Nanodiscs were assembled with the optimized ratio of POPC to MSP1D1 and separated by the gel filtration column Superose 6. (B) The fractions from the peak (*) in (A) were resolved in a 10% SDS gel under non-reducing condition and stained with Coomassie blue staining. (D) GPIb-IX complex was incorporated into excess Nanodiscs and purified by Superose 6 column (continuous line); GPIb-IX complex was mixed only with POPC and analyzed by Superose 6 column (dashed line). (E) The fractions from the peak (**) in (D) were resolved in a 10% SDS gel under non-reducing condition and stained with Coomassie blue staining. Nanodisc elution was monitored by absorbance at 280 nm (A_{280}). The calibrated Stokes diameter scale and void volume for this column are shown at the top of (A) and (D). Negative-stain TEM of empty Nanodiscs (C) and Nanodiscs with GPIb-IX complex (F) with a magnification of 40,000. The scale bar was shown below the image.

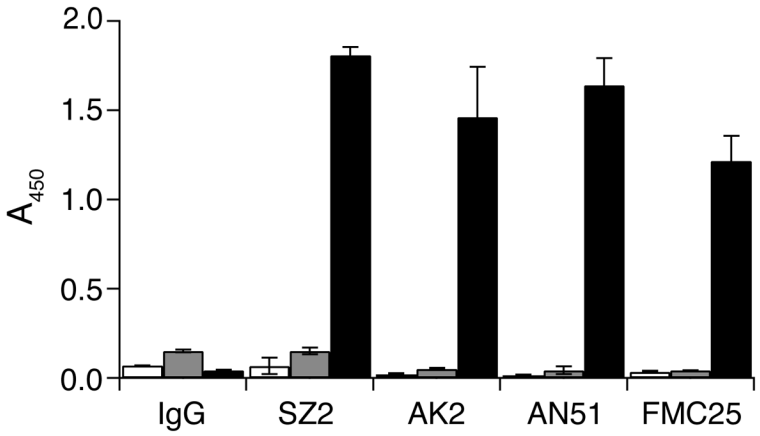

Figure 3. Probing GPIb-IX complex reconstituted in Nanodiscs by conformation-sensitive monoclonal antibodies

1 μg/ml of mouse IgG or antibodies against GPIbα (SZ2, AK2 and AN51) or against GPIX (FMC25) was incubated with immobilized GPIb-IX/ND (■) or empty Nanodiscs (■) or BSA (□). The bound antibodies were detected by ELISA, using HRP-conjugated goat anti-mouse antibody. Absorbance at 450 nm was measured from 3 independent experiments and presented as the mean ± SD.

$watermark-text
$watermark-text
$watermark-text

$watermark-text
$watermark-text
$watermark-text

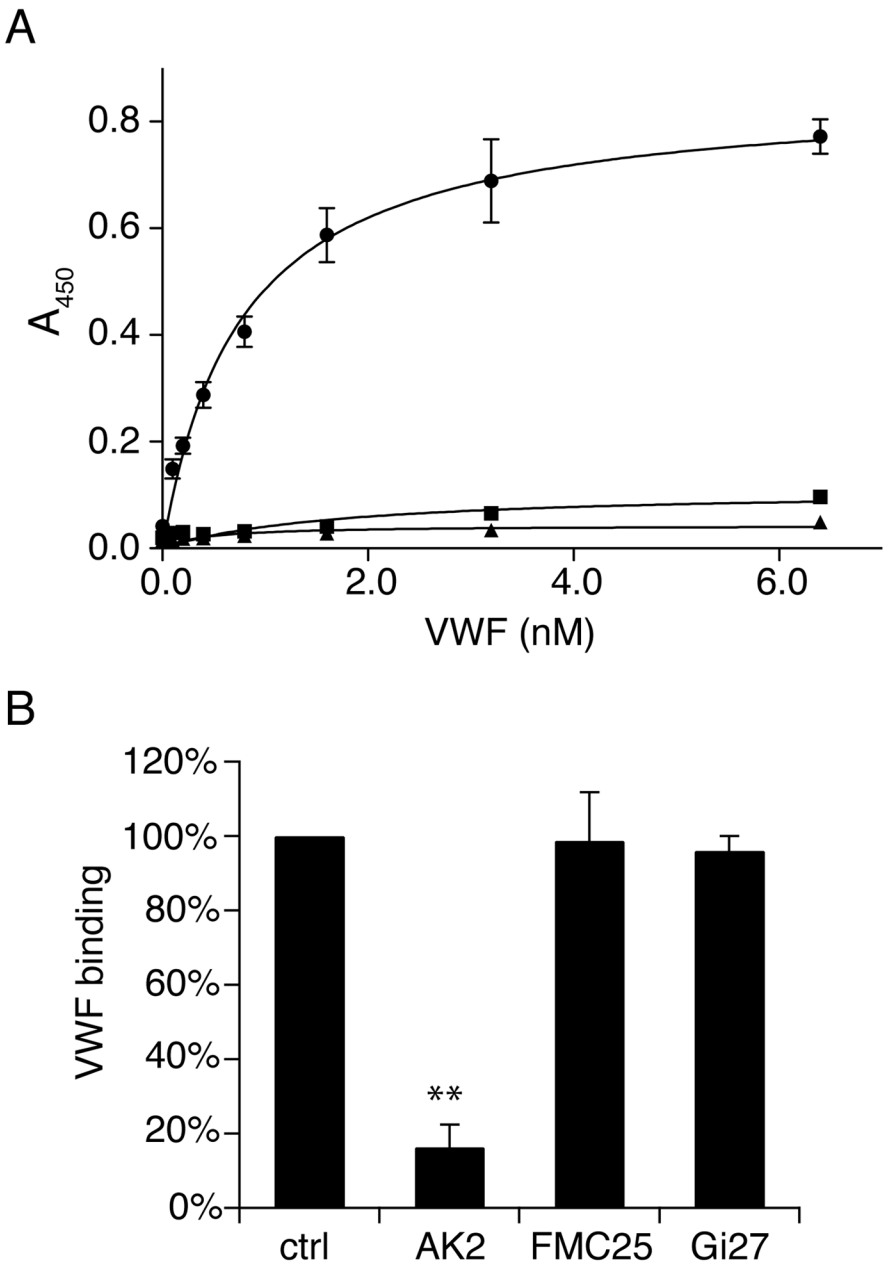

Figure 4. Botrocetin-induced binding of VWF to GPIb-IX reconstituted in Nanodiscs

(A) Botrocetin-induced VWF binding to GPIb-IX in Nanodiscs measured by ELISA. Increasing concentrations of VWF was incubated with immobilized GPIb-IX/ND (●) or empty Nanodiscs (■) or BSA (▲) in the presence of 0.2 U/ml botrocetin. The binding of VWF was determined by rabbit anti-VWF antibody and HRP-conjugated goat anti-rabbit antibody. (B) The effect of monoclonal antibodies against individual subunits of GPIb-IX complex on VWF binding. 10 μg/ml antibodies were pre-incubated with immobilized GPIb-IX/ND before 0.8 nM VWF with 0.2 U/ml botrocetin was added. The bound VWF was detected by HRP-conjugated anti-VWF antibody. Absorbance at 450 nm was measured from 3 independent experiments and presented as the mean ± SD. For some data points, their error bars are smaller than the symbols. One hundred percent in (B) is defined as the binding

of VWF to GPIb-IX/ND in the absence of inhibitory antibodies after subtracting the binding to empty Nanodiscs. Groups were compared using the Student't test. $^{**}P < 0.01$ v.s. control.

$watermark-text

$watermark-text

$watermark-text

$watermark-text
$watermark-text
$watermark-text

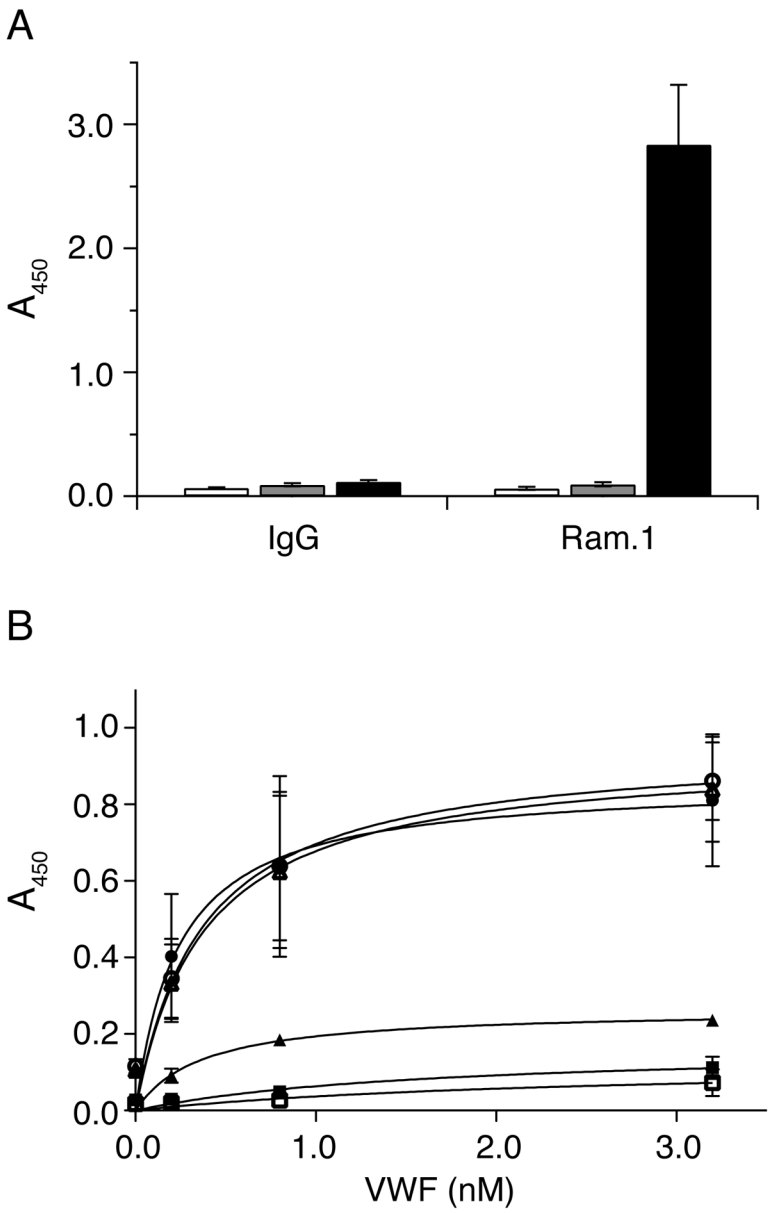

Figure 5. Effect of RAM.1 on the VWF-binding activity of GPIb-IX reconstituted in Nanodiscs

(A) The binding of RAM.1 to GPIb-IX in Nanodiscs. 2 μg/ml rat IgG or RAM.1 was incubated with immobilized GPIb-IX/ND (■) or empty Nanodiscs (■) or BSA (□) and the binding was detected by HRP-conjugated goat anti-rat antibody. (B) The effect of RAM.1 on botrocetin-induced VWF binding to GPIb-IX in Nanodiscs. 10 μg/ml antibodies, rat IgG (○) and RAM.1 (●), mouse IgG (△) and AK2 (▲) were pre-incubated with GPIb-IX/ND-coated wells, and then increasing concentrations of VWF with 0.2 U/ml botrocetin was added. The binding was detected by HRP-conjugated anti-VWF antibody. The addition of VWF with botrocetin to empty Nanodiscs- (■) or BSA- (□) coated wells served as negative controls. Absorbance at 450 nm was measured from 3 independent experiments and presented as the mean ± SD. For some data points, their error bars are smaller than the symbols.

$watermark-text
$watermark-text
$watermark-text

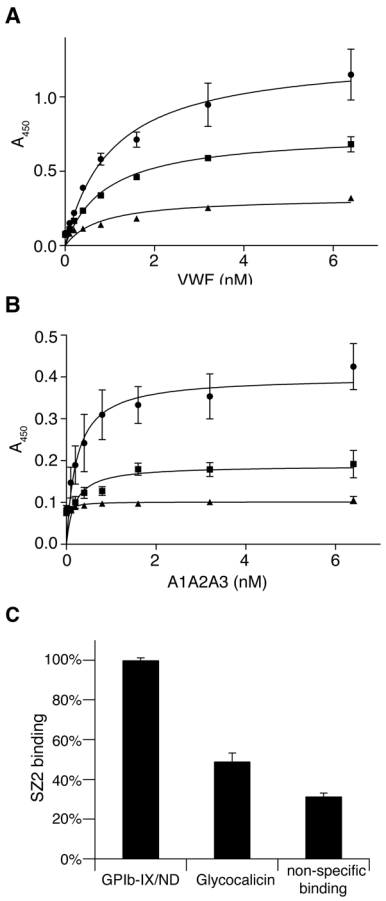

Figure 6. Comparison of ligand-binding activities between GPIb-IX/ND and glycocalicin

4 μg/ml WM23 IgG was immobilized onto microtiter wells to capture GPIb-IX/ND (●) and glycocalicin (■). Empty Nanodiscs (▲) was also added to the WM23-coated wells as a control. (A) 0–6.4 nM full-length VWF or (B) A1A2A3 tri-domains was incubated with GPIb-IX/ND or glycocalicin or control wells in the presence of 0.2 U/ml botrocetin. The binding was detected by anti-VWF antibody and HRP-conjugated secondary antibody. (C) Difference in capturing efficiency. 4 μg/ml WM23 IgG $F(ab')_2$ fragment was coated to microtiter wells to capture GPIb-IX/ND or glycocalicin. Empty Nanodiscs was also added to the wells coated with WM23 $F(ab')_2$ fragment as a control. SZ2 (1 μg/ml) was incubated and detected by HRP-conjugated goat-anti-mouse antibody. "Non-specific binding" is the binding of SZ2 to the control wells. Absorbance at 450 nm was measured from 3 independent experiments and presented as the mean ± SD. For some of the points, the error bars are smaller than the symbols. One hundred percent in (C) is defined as the binding of SZ2 to GPIb-IX/ND captured by WM23 $F(ab')_2$ fragment.